Metabolic Engineering 60 (2020) 110–118

Contents lists available at ScienceDirect

Metabolic Engineering

journal homepage: www.elsevier.com/locate/meteng

Precise promoter integration improves cellulose bioconversion and thermotolerance in *Clostridium cellulolyticum*

Xuanyu Tao[a,1], Tao Xu[a,b,c,1,*], Megan L. Kempher[a], Jiantao Liu[a], Jizhong Zhou[a,d,e,**]

[a] Institute for Environmental Genomics, Department of Microbiology and Plant Biology, and School of Civil Engineering and Environmental Sciences, University of Oklahoma, Norman, OK, USA
[b] Section on Pathophysiology and Molecular Pharmacology, Joslin Diabetes Center, Boston, MA, USA
[c] Department of Microbiology and Immunobiology, Harvard Medical School, Boston, MA, USA
[d] Earth and Environmental Sciences, Lawrence Berkeley National Laboratory, Berkeley, CA, USA
[e] State Key Joint Laboratory of Environment Simulation and Pollution Control, School of Environment, Tsinghua University, Beijing, China

ARTICLE INFO

Keywords:
Promoter integration
Cellulosome
Cellulose degradation
Microbial engineering

ABSTRACT

Lignocellulose has been used for production of sustainable biofuels and value-added chemicals. However, the low-efficiency bioconversion of lignocellulose greatly contributes to a high production cost. Here, we employed CRISPR-Cas9 editing to improve cellulose degradation efficiency by editing a regulatory element of the *cip-cel* gene cluster in *Clostridium cellulolyticum*. Insertion of a synthetic promoter (P4) and an endogenous promoter (P2) in the *mspI*-deficient parental strain (Δ2866) created chromosomal integrants, P4-2866 and P2-2866, respectively. Both engineered strains increased the transcript abundance of downstream polycistronic genes and enhanced *in vitro* cellulolytic activities of isolated cellulosomes. A high cellulose load of 20 g/L suppressed cellulose degradation in the parental strain in the first 150 h fermentation; whereas P4-2866 and P2-2866 hydrolyzed 29% and 53% of the cellulose, respectively. Both engineered strains also demonstrated a greater growth rate and a higher cell biomass yield. Interestingly, the Δ2866 parental strain demonstrated better thermotolerance than the wildtype strain, and promoter insertion further enhanced thermotolerance. Similar improvements in cell growth and cellulose degradation were reproduced by promoter insertion in the wildtype strain and a lactate production-defective mutant (LM). P2 insertion in LM increased ethanol titer by 65%. Together, the editing of regulatory elements of catabolic gene clusters provides new perspectives on improving cellulose bioconversion in microbes.

1. Introduction

Cellulose, as the most abundant renewable bioresource on earth, can be used to produce sustainable valuable products (Jarvis, 2003; Zhang et al., 2006). In order to save cost and improve efficiency for utilization of cellulose, a promising strategy named consolidated bioprocessing (CBP) was proposed, which involves a single microorganism for cellulase production, saccharification, and fermentation in a single step in one bioreactor (Lynd et al., 1991; Zhang et al., 2006). Although there are some CBP-enabling microorganisms able to perform both cellulose hydrolysis and sugar fermentation simultaneously, they need to be engineered with improved cellulose degradation, greater resistance to abiotic and biotic factors, and higher production efficiency (Li et al., 2012b; Lynd et al., 2005). Efficient conversion of cellulose to fermentable sugars is key to reducing the cost during production (Li et al., 2012b; Liao et al., 2016; Zhang et al., 2006).

Clostridium cellulolyticum is a model mesophilic clostridial species, able to convert lignocellulose to ethanol and organic acids (Desvaux, 2005b; Li et al., 2012b, 2014). Like other cellulose-degrading Clostridia, it forms extracellular enzymatic complexes, termed cellulosomes, that degrade crystalline cellulose with greater efficiency than free or non-organized enzymes as a result of the proximal synergism of enzyme reactions (Desvaux, 2005a; Gal et al., 1997). The cellulosome of *C. cellulolyticum* contains a cell surface-anchored scaffoldin and a diversity of carbohydrate-active enzymes. Major cellulosomal components are encoded by a 26 kb *cip-cel* gene cluster. This cluster has 11 genes (*cipC-*

* Corresponding author. Section on Pathophysiology and Molecular Pharmacology, Joslin Diabetes Center, Boston, MA, USA.
** Corresponding author. Institute for Environmental Genomics, Department of Microbiology and Plant Biology, and School of Civil Engineering and Environmental Sciences, University of Oklahoma, Norman, OK, USA.
E-mail addresses: Tao.Xu@joslin.harvard.edu (T. Xu), jzhou@ou.edu (J. Zhou).
[1] These authors contributed equally to this work.

https://doi.org/10.1016/j.ymben.2020.03.013
Received 3 January 2020; Received in revised form 22 March 2020; Accepted 30 March 2020
Available online 12 April 2020

cel48F-cel8C-cel9G-cel9E-orfX-cel9H-cel9J-man5K-cel9M-rgl11Y-cel5N) (Desvaux, 2005a), driven by a single promoter (Maamar et al., 2006). There were two major large transcripts detected when *C. cellulolyticum* was grown on cellulose (Maamar et al., 2006). The most abundant transcript covers the first five genes (*cipC-cel48F-cel8C-cel9G-cel9E*); whereas the other transcript is much lower in abundance and only contains the remaining downstream genes (*cel9H-cel9J-man5K-cel9M-rgl11Y-cel5N*). This difference in transcript abundance can be attributed to site-specific RNA processing and differential resistance of processed RNAs to RNase-mediated degradation (Xu et al., 2015a). As Cel9H, Cel9J, Cel9M, and Cel5N, are endoglucanases that are critical for cellulose solubilization (Blouzard et al., 2010), we hypothesized that improvement in cellulose hydrolysis could be achieved by the manipulation of their expression levels. However, thus far, it has been technically difficult to engineer transcriptional regulatory elements in the native genome of *C. cellulolyticum* (Xu et al., 2015b).

With the development of Cas9 nickase-based genome editing in Clostridia (Xu et al., 2015b), we are now able to tune gene expression by manipulating regulatory systems. Here, we aimed to improve cellulose degradation by inserting constitutively active promoters in front of the *cel9H* gene, by which the transcription of the six downstream genes (*cel9H-cel9J-man5K-cel9M-rgl11Y-cel5N*) can be increased independently of the upstream genes. We systematically characterized the resulting engineered strains from transcriptional, enzymatic, physiological, and morphological aspects. Additionally, since a previous study demonstrated that a 5 °C increase of the fermentation temperature could greatly reduce the cost for fuel ethanol production (Abdel-Banat et al., 2010), and enzymatic assays indicated that the activity of cellulases could be increased when the temperature was increased (Mingardon et al., 2011), we also examined the fitness and thermotolerance of our engineered strains at an elevated temperature. Additionally, we applied the same strategy to other engineered *C. cellulolyticum* strains to test whether their cellulolytic activity and ethanol production could be further improved. Our results demonstrated that a precise promoter insertion is an efficient strategy to modulate the transcriptional abundance of catabolic gene clusters for improving efficiencies of cellulose degradation and end-product formation.

2. Materials and methods

2.1. Bacterial strains and plasmid construction

Strains, plasmids, and primers used in this study were listed in Supplementary Tables S1 and S2, respectively. pCas9n-P4inser-donor and pCas9n-P2inser-donor, for inserting the promoter in the *cip-cel* gene cluster, were constructed as described before (Xu et al., 2015b). First, the predicted P2 promoter, left and right homologous arms, were amplified from wild-type genomic DNA of *C. cellulolyticum* and purified separately. The P4 promoter was synthesized as part of the 9HP4LR and 9HP4RF primers which were used for the amplification of left and right homologous arms. The P4:gRNA cassette containing the 20-bp protospacer was amplified from pCR/8w p4-4 prom4 and pMS-RNA by 3FF, PM9HGRF, PM9HGRR, and 2RR primers. The linear backbone was digested from pFdCas9n-p4-pyrF_w/2kbΔ by KpnI and PvuI. These fragments were assembled using Gibson assembly and the assembled product was transformed into *E. coli* for colony screening and confirmed via Sanger sequencing (Oklahoma Medical Research Foundation). The plasmid for promoter insertion in *C. cellulolyticum* was cured as previous reported (Li et al., 2012b).

2.2. Media and culture conditions

E. coli DH5α strain (Invitrogen) was used for cloning and grown at 37 °C in LB with 35 μg/ml chloramphenicol. Complex modified VM medium supplemented with 2.0 g/L yeast extract was used for general growth and transformation of *C. cellulolyticum* H10 (Li et al., 2012b). Defined modified VM medium containing necessary vitamin solution and mineral solution was used for fermentation and omics experiments (Higashide et al., 2011). *C. cellulolyticum* H10 was cultured with 5 g/L cellobiose or 20 g/L Avicel PH101 crystalline cellulose (Sigma-Aldrich) at 34 °C or 40 °C anaerobically depending on the experiment. Solid VM medium with 1.0% (w/v) of Bacto agar (VWR) and 15 μg/ml thiamphenicol was used for developing *C. cellulolyticum* colonies.

2.3. Transformation

The wild-type *C. cellulolyticum* and Δ2866 parental strain were transformed with corresponding plasmids by electroporation as described previously (Jennert et al., 2000; Li et al., 2012b). For transformation of the wildtype *C. cellulolyticum* strain, plasmid DNA was methylated using MspI Methyltransferase (New England Biolabs, Ipswich, MA) and then purified prior to transformation (Li et al., 2012b).

2.4. Microarray analysis

All *C. cellulolyticum* strains (i.e., Δ2866, P2-2866, P4-2866 and wildtype) were cultivated in defined VM medium with 20 g/L cellulose or 5 g/L cellobiose. Six biological replicates of each strain were collected at mid-exponential growth phase. All samples were centrifuged at 4 °C and 5000 × *g* for 10 min and cell pellets were immediately frozen with liquid nitrogen and then stored at −70 °C for further use. Total RNA was extracted using TRIzol (Invitrogen) and purified using NucleoSpin RNAII kit (Macherey-Nagel) according to the manufacturer's instructions. RNA integrity was examined on agarose gels; RNA purity and concentration were measured with a NanoDrop spectrophotometer.

For microarray hybridization, 13,098 probes (50 nt in length) were designed to cover 94% of the protein encoding genes in *C. cellulolyticum* (Agilent). For each RNA sample, 0.6 μg of total RNA was reverse transcribed to Cyanine-3 labeled cDNA using Reverse Transcriptase III (Invitrogen) using Cyanine 3-labeled dUTP (Thermo Fisher). Genomic DNA (gDNA) was extracted from the control strain using GenElute bacterial genomic DNA kit (Sigma Aldrich) and was labeled by incorporating Cyanine 5-labeled dUTP with Klenow DNA polymerase (New England Biolabs). 1.5 μg of gDNA was used in each gDNA labeling reaction which was used for eight hybridizations. All labeled cDNA and gDNA were purified with QIAquick PCR purification reagents (Qiagen) and SpinSmart columns (Denville Scientific Inc), and then lyophilized for later use. Labeled cDNA and gDNA were mixed in the hybridization master buffer (Agilent) containing 8% formamide, followed with denaturation at 95 °C for 3 min, incubation at 37 °C for 30 min and finally loaded onto an array. Hybridization was carried out at 67 °C and 20 rpm for 22 h. Slides were washed and then scanned using a NimbleGen MS200 scanner (Roche) with the following settings: two-channel scanning, 2 μm scanning resolution, 100% laser strength, 30% gain percentage. Using Agilent Feature Extraction version 11.5, all digital images were manually checked to confirm gridding quality and raw data was extracted.

Microarray data analysis was performed using the limma package in R (Ritchie et al., 2015). First, probes with both qualified green and red signals were screened (single-to-noise ratio > 2, signal-to-background ratio > 1.3, coefficient of variation < 0.8, minimal gMeansigal > 150, and minimal rMeansignal > 50) (He and Zhou, 2008). Second, the mean signal of each probe was applied to background correction by subtraction, within-array normalization by loess, and then between-array normalization by quantile. Third, using the normalized data, gene probes with significantly different expression levels were identified using limma's linear model and then evaluated by empirical Bayes methods. The expression level of each gene was calculated by averaging the values of qualified probes only if half or more probes of this gene were qualified. In this study, differentially expressed genes (DEGs) refer to genes with a log2 fold-change above 1 (or below −1) and an

adjusted p value < 0.05. Venn diagram graphs were generated with the online tool (http://bioinformatics.psb.ugent.be/webtools/Venn/). Blast2go was used for GO enrichment analysis with Fisher's exact test ($p < 0.01$, two sided) (Conesa et al., 2005). PCA analysis was conducted with the prcomp function in R using the normalized data. The functional enrichment analysis was performed using ClueGO v 2.5.5 and CluePedia v 1.5.5 (Bindea et al., 2009, 2013). The significance of the terms and groups was calculated using ClueGo. The P value was calculated using a two-sided minimal-likelihood test and corrected using the Benjamini-Hochberg method. The final enrichment network was visualized using Cytoscape v3.7.2.

2.5. Measurements of FPase, Avicelase, CMCase and xylanase activities

The activities of Avicelase and CMCase were determined as described previously (Zhang et al., 2009). The cellulosome fraction was isolated from 200 ml cellulose-grown culture at mid-exponential growth phase. Cell cultures were filtered with glassfiber paper to remove media. Retained cellulose-associated components were firstly washed three times on the glassfiber with 50 ml of 50 mM PBS buffer, then washed three times with 50 ml of 25 mM PBS buffer. Finally, cellulose-associated cellulases, mainly cellulosomes, were eluted with 20 ml of sterile water and centrifuged to discard insoluble material before applying to a protein concentrator with a 5 kDa ultracentrifuge membrane. Protein samples were mixed with an equal amount of 40 mM Tris-maleate buffer (with 4 mM Ca^{2+}) with 50% glycerol and then stored at −20 °C. Protein concentration was determined by a BCA assay kit (Thermo Fisher Scientific).

Total cellulase activity was monitored using a filter paper assay. For each reaction, 1 ml Tris-maleate buffer was pre-incubated with a 25 mg filter paper disc at 37 °C for 20 min before adding a mixture of 200 μg protein and 5 μl of diluted β-glucosidase (1:250) to initiate the reaction. Reaction controls were generated by using the same amount of boiled protein mixtures. Reactions were carried out at 37 °C and 200 μl of reaction products were sampled at 0, 3, 8.5, 22 h. After centrifugation, the concentration of released reducing sugars in the supernatant was determined by the DNS method (Miller, 1959). Avicelase was measured while shaking with 2% Avicel that was washed with Tris-maleate buffer. CMCase activity and Xylanase activity were measured with 1.25% CMC and beechwood xylan, respectively, with 10 μg protein used in assays. 120 μl of DNS reagent was mixed with 40 μl reaction product in PCR strip tubes and incubated at 98 °C for 10 min in a thermocycler. A 140 μl aliquot of each sample was transferred to a 96 well plate and the absorbance at 544 nM was measured using an Optima plate reader.

2.6. Scanning electron microscopy (SEM)

All *C. cellulolyticum* strains (Δ2866, P2-2866 and P4-2866) were cultivated in defined VM medium with 20 g/L cellulose or 5 g/L cellobiose. At the mid-exponential growth phase, cell pellets from each strain were collected by centrifugation at 5000 g for fixation. Cell pellets were immersed in 4% glutaraldehyde in 0.1 M PBS buffer (pH 7.4). After incubation at 4 °C overnight, all samples were washed three times with PBS, and immersed in 1% OsO_4 at 4 °C for 1 h. After the post-fixation, de-ionized water was used to remove all traces of fixative and buffer solutions. Dehydration was performed by immersing all washed samples for 10 min sequentially in 25%, 50%, 70%, 85%, 95%, and 100% ethanol to remove all traces of water. Samples were air dried and critical point dry for 10 min after dehydration. Samples then were mounted onto SEM stubs and a dab of silver was applied. Finally, all samples were coated with ~5 nm AuPd. The number of cell surface protuberances was quantified for each strain (Δ2866, P2-2866, and P4-2866) when grown on cellulose or cellobiose. Cells were randomly chosen from different views of SEM images to count protuberances. Statistical differences in the number of protuberances between parent strain and engineered strains were determined using one-way ANOVA with permutation test (PERM-ANOVA) using the lmPerm package in R (Venables and Ripley, 2013).

2.7. Genomic DNA sequencing

Genomic DNA of P4-2866 and P2-2866 was extracted using the GenElute™ Bacterial Genomic DNA Kit. Libraries for gDNA sequencing were constructed using a KAPA DNA Library Preparation kit (Kapa Biosystems) following instructions and then sequenced using Illumina MiSeq platform by the Miseq Reagent Kit V2 (2 × 250 bp).

2.8. Measurement of cell growth, fermentation products, and remaining cellulose

All *C. cellulolyticum* strains were revived in complex VM medium with 5 g/L cellobiose and then transferred to defined VM media. The cellobiose-grown cultures at an OD_{600} of 0.5–0.6 were used to inoculate 50 ml of defined VM media containing 20 g/L Avicel PH101 crystalline cellulose. Each strain had three biological replicates. During growth, 1 ml of cell culture was sampled at each time point and then stored at −80 °C for future determination of cell biomass, metabolites, and remaining cellulose. Growth curves for each sample grown on cellulose was estimated by total protein measurement (Li et al., 2012b). High-performance liquid chromatography (HPLC) was used to measure the major fermentation products (lactate, acetate, and ethanol) and soluble sugars (cellobiose and glucose) in the supernatant of spent medium (Li et al., 2012b). The specific rate of product formation was calculated as previously described (Desvaux et al., 2000). The remaining cellulose in the medium was measured by the phenol-sulfuric acid method (Hemme et al., 2011).

3. Results

3.1. Targeted promoter insertion in the cip-cel gene cluster enhanced the cellulolytic activity of isolated cellulosomal complexes

To test whether promoter insertion into the *cip-cel* gene cluster would promote cellulose degradation, we selected two constitutive promoters, a synthetic promoter named P4 and an endogenous promoter named P2. P4 promoter is a mini promoter from our previous study (Xu et al., 2015b), which was used to drive the gRNA cassette expression in our Cas9 genetic editing system for *C. cellulolyticum*. P2 is a predicted promoter of the Ccel_2112 gene, which encodes an extracellular solute-binding protein family 1 and was previously shown to be transcribed at a higher level in cells grown with cellulose and corn over cellobiose (Xu et al., 2015a). For each promoter insertion, we constructed an all-in-one vector for Cas9 nickase-based genome editing, which requires co-expression of Cas9 nickase and a customized gRNA, as well as homologous regions that sandwich the promoter sequence (Fig. 1A). The corresponding engineered strains, P4-2866 and P2-2866, were generated in the parental strain (Δ2866) which is a *mspI*-deficient mutant that was originally engineered to improve transformation efficiency by allowing non-methylated DNA transformation (Cui et al., 2012). We performed whole genome resequencing to confirm precise promoter insertion without any off-target insertion in the genome.

Microarray-based transcriptomic analysis revealed a large increase in the transcript abundance of downstream polycistronic genes driven by either promoter. Compared with Δ2866, when grown on cellulose, cellulase genes downstream of the inserted promoter including *cel9J*, *cel9M*, and *cel5N,* were dramatically upregulated in both P4-2866 and P2-2866, but to a greater extent in P4-2866 (Fig. 1B). A similar trend was also observed when grown on cellobiose suggesting that the P4 promoter led to greater expression than the P2 promoter (Fig. 1B). However, the transcript levels of downstream genes in both promoter integrants were not significantly different between cellulose and

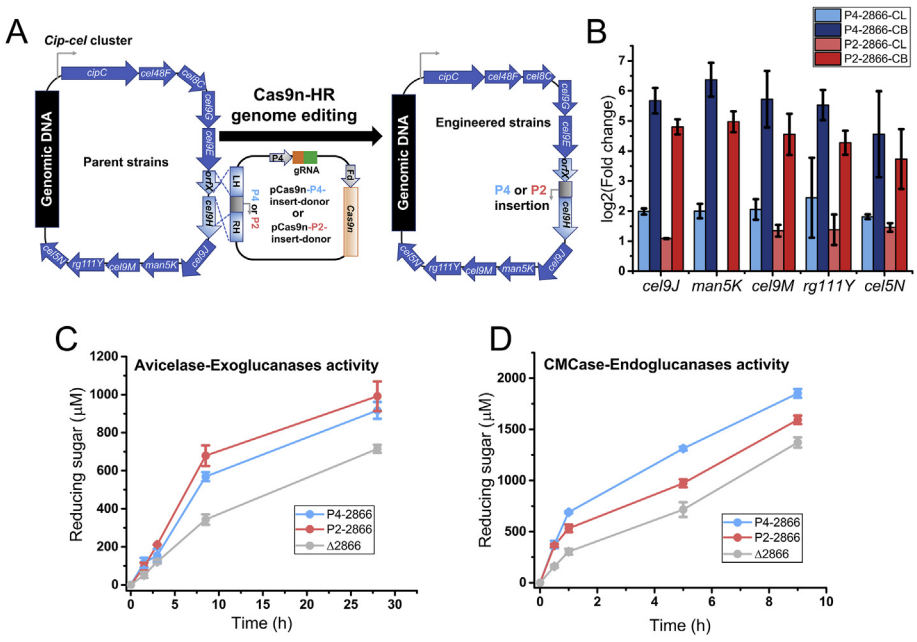

Fig. 1. One-step promoter integration increased expression of downstream genes in the *cip-cel* gene cluster and improved *in vitro* cellulolytic features. (A) An overview of the Cas9 nickase-based genome editing in *C. cellulolyticum*. Plasmids pCas9n-P4insert-donor and pCas9n-P2insert-donor were used for the synthetic P4 (blue) and predicted P2 (red) promoter insertion in the *cip-cel* gene cluster between *orfX* and *cel9H* in the genetic background of Δ2866, wild-type (WT), and lactate production defective strain (LM). (B) Promoter integration increased the transcription of downstream polycistronic genes (*cel9H-cel9J-man5K-cel9M-rgl11Y-cel5N*). Fold change was determined between either P4-2866 and Δ2866 or P2-2866 and Δ2866. All strains were grown on defined VM medium with 20 g/L cellulose (CL) or 5 g/L cellobiose (CB). Data are presented as the mean of six biological replicates and error bars represent standard deviation (SD). (C) *In vitro* enzymatic assay measuring the activity of exoglucanases of Avicelase in isolated cellulosomes from P4-2866, P2-2866, and Δ2866. (D) *In vitro* enzymatic assay measuring the activity of endoglucanases of CMCase in isolated cellulosomes from P4-2866, P2-2866 and Δ2866. Data for (C) and (D) are presented as the mean of three biological replicates and error bars represent SD. (For interpretation of the references to colour in this figure legend, the reader is referred to the Web version of this article.)

cellobiose, indicating the promoters were not cellulose-specific. In addition, promoter insertion also affected the expression of other genes located across the genome and the P4 promoter presented a more profound impact than the P2 promoter, irrespective of using cellobiose or cellulose as a carbon source (Fig. S1A). PCA analysis indicated that the gene expression profiles were different for P4-2866, P2-2866, and Δ2866 strains when grown on cellulose but not on cellobiose (Fig. S1B). This indicates that some genes were affected by the inserted promoter activity but only during growth on cellulose.

To test if promoter insertion altered cellulolytic activity, we isolated cellulosome fractions from cultures grown on cellulose and analyzed cellulosomal composition and enzyme activity. SDS-PAGE analysis showed that the engineered strains significantly changed cellulosomal components, which is in agreement with the observed increased transcriptional abundance (Fig. S2). It is known that efficient cellulose degradation relies on synergistic reactions of multiple enzymes, such as endoglucanase, exoglucanase, and β-glucosidase (Asztalos et al., 2012). We found cellulosomes from both engineered strains dramatically improved the activity of exoglucanases and endoglucanases when compared with isolated cellulosomes from the Δ2866 parental strain (Fig. 1C & D). Therefore, targeted promoter insertion enhanced gene expression at both transcriptional and enzymatic levels.

3.2. Engineered strains presented notable changes in cell morphology

During screening of engineered strains, we observed that P4-2866 formed visible cotton-like aggregates when statically cultured on cellobiose. This morphology was distinct from planktonic cell suspensions of other strains (wildtype, P2-2866, and Δ2866). Scanning electron microscopy revealed that, irrespective of using cellobiose or cellulose as the carbon source, P4-2866 had an altered cell arrangement changing from typical single rods to cell chains (Fig. 2 & Fig. S3). The same morphological change was observed with other randomly picked P4-2866 integrants. Whole genome sequencing confirmed that no other mutations were present and that the change in morphology could be attributed to the insertion of the P4 promoter. Neither engineered strains presented a substantial change in cell diameter or length relative to Δ2866.

Cellulosomes are further organized to form protuberances on cell surface as observed in *Clostridium thermocellum* and *Clostridium cellulovorans* (Bayer and Lamed, 1986; Tachaapaikoon et al., 2012; Tamaru et al., 2010); however, it remains inconclusive in C. *cellulolyticum* (Desvaux, 2005b; Ferdinand et al., 2013). By closely examining SEM images, we found P2-2866 and P4-2866 displayed 7-fold more protuberances than Δ2866 on cellulose and 5-fold more on cellobiose (Fig. 2 & Fig. S3). It is possible that promoter insertion or increased expression of cellulases influenced the organization and localization of cellulosome complexes on cell surface, and further studies will be necessary to confirm this.

3.3. Engineered strains improved conversion of cellulose to end products

We compared cell growth and metabolism of P4-2866, P2-2866, and Δ2866 in defined VM media with 20 g/L Avicel cellulose. P4-2866 and P2-2866 not only had shorter doubling times, which was two-fold faster than Δ2866, but both strains also had increased cell biomass of 60% and 52%, respectively (Table 1 & Fig. 3A). At 150 h, P2-2866 and P4-2866 entered stationary phase and degraded 53% and 29% of cellulose, respectively; whereas Δ2866 used very little cellulose, indicative of strong growth suppression (Fig. 3B). Although the engineered strains did not enhance the final titers of major end products (lactate, acetate, and ethanol) at 300 h (Figure S4A, 4B & 4C), they demonstrated an efficient product formation within a shorter fermentation time (Fig. 3C), which is in line with their faster growth profiles. Also, P2-2866 accumulated more soluble sugars than Δ2866 (Figs. S4D and 4E). More specifically, glucose and cellobiose increased by 52% and 38%, respectively.

As the rate of an enzyme (cellulase)-catalyzed reaction increases as the temperature is elevated within an acceptable range (Mingardon et al., 2011), we attempted to test the effect of growth temperature on cellulose conversion for our engineered strains. Given that the upper limit temperature for *C. cellulolyticum* growth is 45 °C (Desvaux, 2005b), we increased the growth temperature from 34 °C to 40 °C. In general, both engineered strains and Δ2866 had significantly increased doubling times when grown at 40 °C, along with a slightly reduced cell biomass (Table 1 & Fig. 3D). Surprisingly, at the entry of stationary phase (150 h), P4-2866 degraded up to 51% cellulose, which is a dramatic improvement when compared to 29% at 34 °C (Fig. 3B & E). The elevated growth temperature did not affect the ability of P2-2866 to degrade cellulose but almost abolished the ability of Δ2866 to use

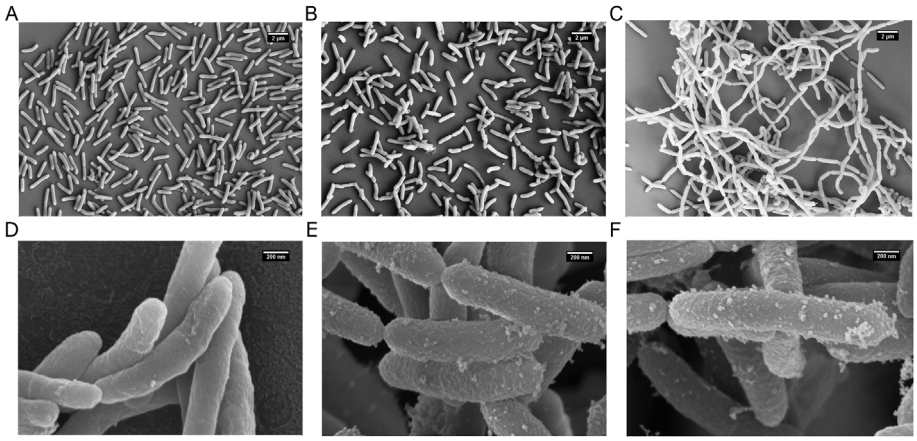

Fig. 2. Promoter integrants altered cell morphology. SEM images of (A) Δ2866 grown on 5 g/L cellobiose; (B) P2-2866 grown on 5 g/L cellobiose; (C) P4-2866 grown on 5 g/L cellobiose; (D) Δ2866 grown on 20 g/L cellulose; (E) P2-2866 grown on 20 g/L cellulose; (F) P4-2866 grown on 20 g/L cellulose.

Table 1
Doubling time (h) [a] of strains grown on 20 g/L cellulose at 34 °C or 40 °C.

Strains	34 °C	40 °C
P4-2866	19.3 ± 1.6	23.9 ± 1.8
P2-2866	17.3 ± 0.3	25.8 ± 3.9
Δ2866	34.7 ± 3.6	53.4 ± 1.9
WT	17.8 ± 3.2	64.7 ± 9.6
P2-WT	13.7 ± 0.4	N/A
P4-LM	33.8 ± 3.4	N/A
P2–LM	28.8 ± 2.3	N/A
LM	38.0 ± 3.8	N/A

[a] The doubling time was determined as the mean of three biological replicates ± standard deviation.

cellulose (Fig. 3E) within 150 h fermentation. Both engineered strains maintained an efficient formation of end products at 40 °C, with much higher yields than the parental strain within 150 h (Fig. 3F); P4-2866 even had a better metabolic performance than P2-2866 (Figs. 3F, S5A, S5B & S5C). Interestingly, lactate titers of P4-2866 and P2-2866 were increased by 10% and 23% when the growth temperature was elevated from 34 °C to 40 °C (Figs. S4B and S5B), suggesting that a higher growth temperature promoted lactate formation in the engineered strains. In addition, P2-2866 accumulated more soluble sugars than Δ2866 at 40 °C, with glucose and cellobiose increased by 55% and 45%, respectively (Figs. S5D and S5E). This is consistent with the previous observations at 34 °C.

3.4. The Δ2866 parental strain conferred the strongest thermotolerance for cellulose degradation

We also compared cellulose degradation between the engineered strains and WT when grown at 34 °C and 40 °C. In general, WT outperformed P4-2866, P2-2866, and Δ2866 in cellulose degradation, ethanol production, and accumulation of soluble sugars at 34 °C

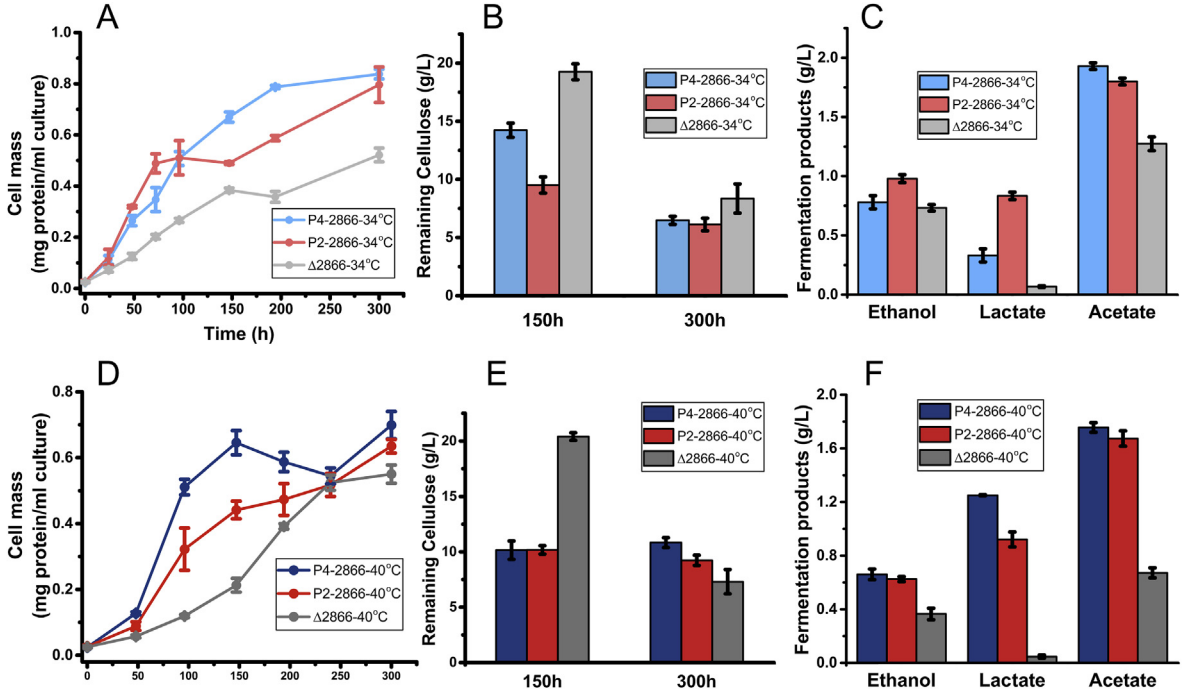

Fig. 3. Promoter integrants improved cell growth and the conversion efficiency of cellulose. Growth profiles of P4-2866, P2-2866 and Δ2866 grown at 34 °C (A) and 40 °C (D). Residual cellulose after 150 h or 300 h fermentation at 34 °C (B) and 40 °C (E). Titers of primary products after 150 h fermentation at 34 °C (C) and 40 °C (F). Data are presented as the mean of three biological replicates and error bars represent SD.

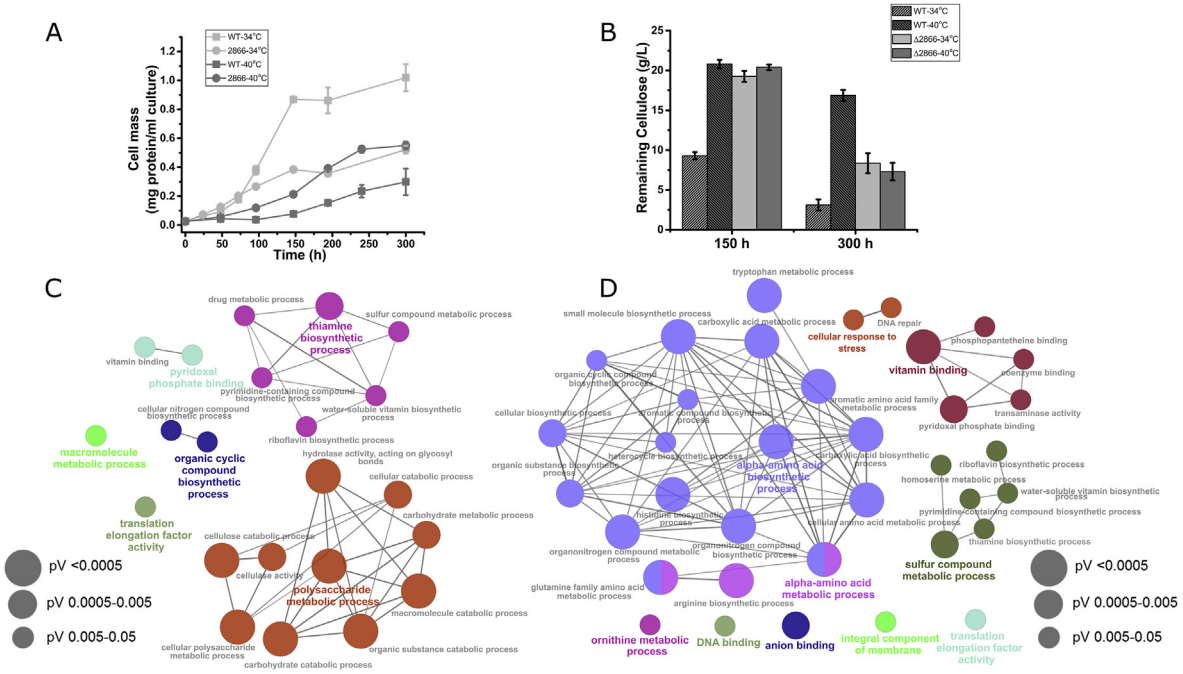

Fig. 4. Δ2866 outperformed WT in growth and cellulose degradation at an elevated temperature. (A) Growth profiles of WT and Δ2866 grown on 20 g/L cellulose at 34 °C and 40 °C. (B) The amount of residual cellulose after 150 h or 300 h fermentation for WT and Δ2866 at 34 °C and 40 °C. Data are presented as the mean of three biological replicates and error bars represent SD. (C and D). Enrichment map of gene ontology (GO) terms in differentially expressed genes (DEGs) between Δ2866 and WT when grown on 20 g/L cellulose at 34 °C (C) and 40 °C (D). Only GO terms with Bonferroni-Hochberg corrected pV < 0.05 are displayed. Term enrichment significance is represented by circle size and the leading group term was based on the highest significance.

(Figs. 3, 4A, 4B & S6). However, acetate production was lower in WT (Fig. S6C). At 40 °C, it is notable that the elevated growth temperature severely inhibited WT growth on 20 g/L cellulose, with a 71% decrease in cell mass yield and only 16% cellulose used in 300 h fermentation when compared to growth at 34 °C (Fig. 4A & B) and was accompanied by low production of all primary end products and little accumulation of soluble sugars (Fig. S6). In contrast, Δ2866 and the engineered strains demonstrated nearly normal cell growth at 40 °C and even slightly improved cellulose utilization (Figs. 3, 4A and 4B). These distinct differences suggested that *mspI* disruption in Δ2866 may have improved the thermotolerance of *C. cellulolyticum* when utilizing cellulose.

To better understand the altered thermotolerance, we monitored transcriptional changes between Δ2866 and WT at both 34 °C and 40 °C. A functional enrichment analysis of the differentially expressed genes (DEGs) found 22 GO terms significantly enriched between these two strains at 34 °C, half of which were associated with polysaccharide metabolism, such as cellulose catabolic process and cellulase activity (Fig. 4C). It is notable that 83% of the DEGs involved in polysaccharide metabolic processes were downregulated in Δ2866 (Supplementary fold change table) at 34 °C, especially those located in the *cip-cel* and *xyl-doc* gene clusters (Fig. 4C & Fig. S7). This may explain why Δ2866 had a lower efficiency of cellulose degradation than WT at 34 °C. In comparison, there were 38 GO terms significantly enriched between Δ2866 and WT at 40 °C and these were mainly involved in cellular response to stress, amino acid metabolism, and vitamin biosynthetic process (Fig. 4D). 11 of the 13 DEGs associated with stress response and DNA repair processes were upregulated in Δ2866 at 40 °C (Supplementary fold change table). In addition, the heat shock protein Hsp20 gene (Ccel_2938) had 3.4 folds increased expression in Δ2866. These upregulated genes in Δ2866 at 40 °C presumably conferred better thermotolerance for Δ2866.

In response to the elevated growth temperature, WT and Δ2866 had transcriptional changes in 276 and 135 genes, respectively. There were no GO terms significantly enriched for the DEGs (34 °C compared to 40 °C) in WT (Fig. S8); whereas DEGs (34 °C compared to 40 °C) in Δ2866 had a significant enrichment in bacterial-type flagellum filament, flagellum-dependent cell motility, bacterial-type flagellum assembly, and ABC transporter complex (Fig. S9). This suggested that the loss of the *mspI* gene in Δ2866 made bacterial flagellum associated functions more susceptible to growth temperature.

3.5. Promoter insertion in other genetic backgrounds also improved microbial physiology

As the WT strain outperformed Δ2866 in cellulose degradation and ethanol production at 34 °C (Figs. 4B and S6), we attempted to insert P4 and P2 promoters into the WT strain at the same locus. However, we only successfully produced the P2 integrant (P2-WT). Consistently, we found P2-WT had a shortened doubling time and an increased maximum cell biomass compared to WT when grown on 20 g/L cellulose at 34 °C (Table 1 & Fig. 5A). P2-WT had a higher cellulose degradation efficiency than WT with 50% of cellulose was degraded by P2-WT versus 15% by WT within 69 h of fermentation (Fig. 5B). Consistently, higher titers of end products were produced by P2-WT within 69 h fermentation (Fig. 5C). As for the final titers, P2-WT produced more acetate but less ethanol than WT, indicating that P2-WT preferentially produced acetate as opposed to ethanol (Fig. S10). Moreover, P2-WT accumulated more soluble sugars than WT as glucose and cellobiose were increased by 35% and 6%, respectively in P2-WT after 300 h fermentation (Figs. S10D and S10E).

The P4 and P2 promoters were also inserted into our previous LM (Δ*ldh*/*mdh*) strain which does not produce lactate but produces more ethanol than WT (Li et al., 2012b). Similarly, the resulting strains, P4-LM and P2-LM, had a shorter doubling time, increased cell biomass, and more efficient cellulose degradation than the parental LM (Table 1 & Fig. 5D and E). After 336 h fermentation, ethanol production by P4-LM and P2-LM was increased by 22% and 68%, respectively (Fig. 5F); like LM, both P4-LM and P2-LM did not accumulate glucose or cellobiose. In sum, all of our engineered strains, regardless of genetic background,

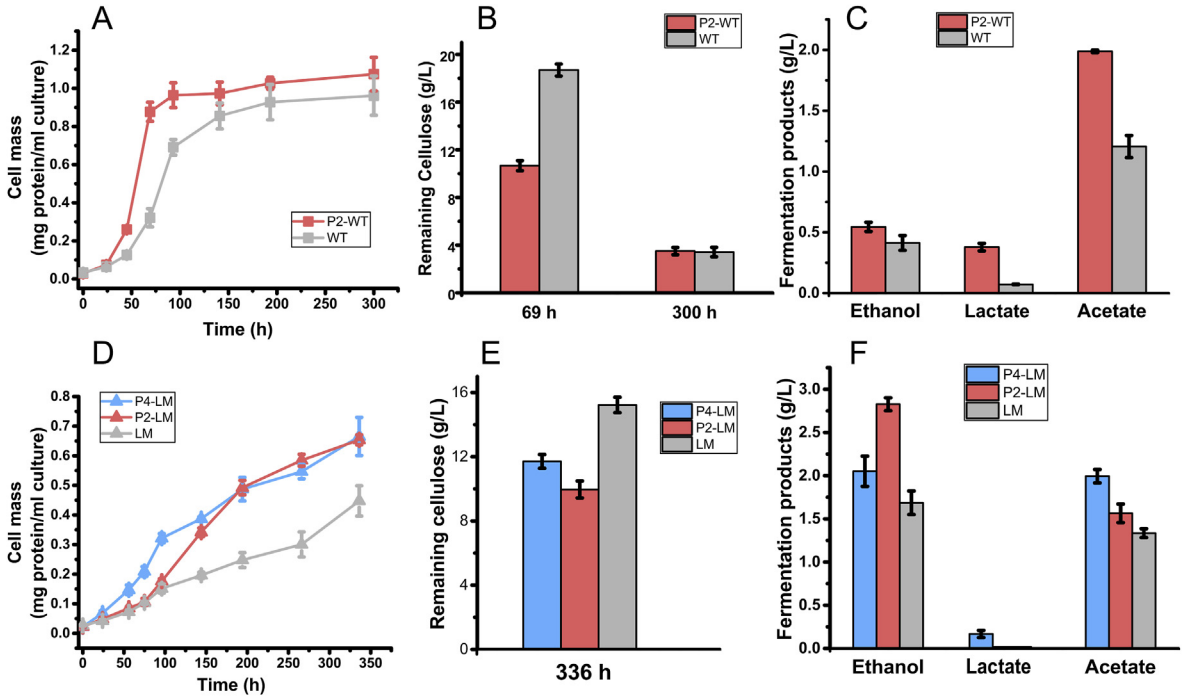

Fig. 5. Targeted promoter insertion in WT and LM enhanced cell growth and the conversion efficiency of cellulose. (A) Growth profiles of P2-WT and WT. (B) Residual cellulose after 69 h and 300 h fermentation by P2-WT and WT. (C) Fermentation products profiles after 69 h fermentation with P2-WT and WT. (D) Growth profiles of P4-LM, P2-LM, and LM. (E) Residual cellulose after 336 h fermentation with P4-LM, P2-LM and LM. (F) Fermentation products profiles at the end time point (336 h) for P4-LM, P2-LM, and LM. Data are presented as the mean of three biological replicates and error bars represent SD.

consistently demonstrated that promoter insertion improved growth rate, maximum cell biomass, efficiencies of cellulose degradation and end-product formation.

4. Discussion

C. cellulolyticum is a CBP candidate and has been engineered for efficient cellulose degradation and biosynthesis of valuable products by both the introduction of heterologous genes and targeted gene inactivation (Guedon et al., 2002; Li et al., 2012b, 2014). However, traditional genome editing approaches suffer from various technical limitations that affect our ability to edit *C. cellulolyticum* for metabolic engineering purposes. To our knowledge, increasing native cellulase expression by rewiring regulatory elements has never been reported in cellulolytic Clostridia. In this study, chromosomal integration of promoters (P4 or P2) improved physiological features of Δ2866, WT, and LM strains, including growth rate, maximum cell biomass, cellulose degradation efficiency, and efficiency of formation of end products. Although engineered strains, such as P4-2866, P2-2866, and P2-WT, did not improve the production rates of all end-fermentation products, such as ethanol (Table 2), their higher growth rate and increased cell biomass dramatically enhanced the efficiency of cellulose bioconversion (Fig. 3C, F & 5C), which therefore shortens the duration of fermentation and promotes equipment effectiveness.

Gene expression analyses with microarray indicated that the P4 promoter had a stronger activity than the P2 promoter (Fig. 1B). In addition to increasing the expression of downstream cellulase genes, the P4 promoter, which is only 60 bp in length, caused many more transcriptional changes than the P2 promoter and a staggering change in cell morphology (the formation of cell chains), irrespective of carbon source (Fig. 2, Figs. S1 and S3). SEM observations indicated that daughter cells formed but failed to properly segregate. This could have resulted from the down-regulation of two cell wall hydrolase genes in cellobiose-grown P4-2866, Ccel_2890 (2.5-fold decrease) and Ccel_2941 (2-fold decrease). The transcriptional change of Ccel_2491 remained

Table 2
Average specific rates[a] of product formation for strains grown in defined VM medium with 20 g/L cellulose at 34 °C.

	q value (μmol [g of cells]$^{-1}$ h^{-1}) for:		
Strains	EtOH	Lactate	Acetate
P4-2866	185.50 ± 1.58	33.85 ± 2.60	322.41 ± 9.17
P2-2866	234.23 ± 7.32	79.34 ± 2.23	429.52 ± 7.25
Δ2866	319.37 ± 6.91	31.26 ± 0.92	356.63 ± 10.30
P2-WT	240.54 ± 6.70	66.65 ± 5.32	272.98 ± 27.40
WT	398.00 ± 14.01	38.08 ± 0.67	237.86 ± 11.80
P4-LM	252.13 ± 19.16	18.75 ± 6.12	231.60 ± 3.64
P2-LM	324.71 ± 21.60	0.00	183.13 ± 10.92
LM	226.51 ± 16.79	0.00	133.93 ± 12.70

[a] The specific rates were determined as the mean of three biological replicates ± standard deviation.

when P4-2866 was grown on cellulose. Other genes involved in cell wall biogenesis were also downregulated in P4-2866, especially when grown on cellobiose. How the insertion of the P4 promoter in the *cip-cel* gene cluster influenced the expression of the cell wall genes will be further investigated in the future. A recent study found that self-induced mechanical stress can trigger the formation of biofilm in *E. coli* (Chu et al., 2018). It is possible that the stronger promoter activity may have caused a stressful burden during RNA transcription and protein synthesis, which then led to the formation of cell chains in P4-2866. Although P2-2866 presented faster cell growth and more efficient cellulose bioconversion than P4-2866 at 34 °C, P4-2866 outperformed P2-2866 at an elevated temperature (40 °C). Whether the formation of cell chain in P4-2866 contributes to its thermotolerance is an interesting question that we will investigate in future experiments.

Although we were unable to generate a P4 integrant in the WT background, which is most likely due to a heavy translational burden on cell resources, the resulting P2-WT strain demonstrated a faster growth rate and cellulose degradation resulted in higher concentrations of soluble sugars accumulated when compared to WT. For instance, glucose and cellobiose were 0.68 g/L and 2.14 g/L in P2-WT while only

0.15 g/L and 0.92 g/L in WT after 141 h fermentation (Figs. S10D and S10E). The efficient accumulation of soluble sugars could be utilized in the future for co-culturing with sugar consuming bacteria (e.g. *Clostridium beijerinckii*) to diversify end products and promote carbon utilization. In addition, we found P2-WT preferentially produced more acetate accompanied with a lower production of ethanol when compared to WT (Fig. S10C). This is in line with the previous observation that increasing cellobiose diverts most carbon flux towards acetate formation (Giallo et al., 1983; Guedon et al., 1999; Payot et al., 1998).

Although previous *in vitro* experiments indicated that a higher temperature (30–60 °C) could increase the activity of cellulases from *C. cellulolyticum* (Mingardon et al., 2011), we did not observe significant improvement by the WT strain in cell-based cellulose utilization experiments at an elevated temperature. Δ2866 and its derived engineered strains (P4-2866 and P2-2866) grew much better than WT at an elevated temperature. Previous studies have shown that heat shock proteins are involved in temperature resistance (Arsène et al., 2000; Chhabra et al., 2006), and it has been reported that *E. coli* cells expressing HSP20 protein from *S. solfataricus* gained greater thermotolerance in response to temperature stress (50 °C) (Li et al., 2012a). The increased expression of the *hsp20* gene (Ccel_2938) in Δ2866 may have contributed to better thermotolerance. In addition to heat shock proteins, it has also been reported that thermotolerant genes involved in membrane formation/stabilization, DNA repair, and transmembrane transportation, were required for growth of *Acetobacter tropicalis* (Soemphol et al., 2011), *E. coli* (Murata et al., 2011) and *Zymomonas mobilis* (Charoensuk et al., 2017) at a high temperature. Our functional enrichment analysis also found that GO terms, such as cellular response to stress, DNA repair, and integral components of the membrane, were significantly enriched between Δ2866 and WT at 40 °C (Fig. 4D). 85% of the DEGs associated with DNA repair, recombination repair, and base-excision repair, were upregulated in Δ2866 and 50% of the DEGs in integral membrane component category had increased expression. Therefore, these DEGs could be involved in repair of any heat-induced DNA damage and stabilization of the membrane, which may help to confer the improved thermotolerance observed for Δ2866 compared to WT. Although it is believed that the restriction-modification (RM) system in bacteria plays a role in stress response (Vasu and Nagaraja, 2013), exactly how the loss of the MpsI endonuclease influenced the expression of the heat shock protein gene and other thermotolerant genes needs to be further investigated in future studies. Considering the Ccel_2866 gene, encoding the MspI endonuclease, belongs to the RM system in *C. cellulolyticum*, *mspI* inactivation might allow for the existence or accumulation of unmethylated CCGG DNA islands across the genome. Changes in methylation status could affect RNA transcription and explain the broad transcriptional impacts on many genes, some of which are associated with carbon metabolism and stress response. This possibility will be further investigated in future work.

In conclusion, one-step targeted promoter insertion in the *cip-cel* gene cluster was demonstrated to be a useful strategy for improving cellulose utilization and end-product formation, which can be applied in other bacteria with similar cellulosome-producing or other biosynthetic systems. We found that inactivation of the *mspI* gene improved thermotolerance in *C. cellulolyticum*, which was further enhanced by the insertion of the P4 and P2 promoters. This feature is an advantage for heat-producing microbial fermentation and high temperature-demanding production that usually requires a strong thermotolerance (Abdel-Banat et al., 2010; Hendriks and Zeeman, 2009). Together, these findings provide new perspectives on how to reduce the cost of industrial fermentation processes and enhance the efficiency of cellulolytic bacteria on cellulose conversion.

Declaration of competing interest

The authors declare no conflict of interest.

Acknowledgement

This work was supported by the Office of the Vice President for Research at the University of Oklahoma. We thank members of the Zhou laboratory for help in the project. We also appreciate the help of Dr. Preston Larson for the SEM assay.

Appendix A. Supplementary data

Supplementary data to this article can be found online at https://doi.org/10.1016/j.ymben.2020.03.013.

Authors' contributions

T.X., and X.T. designed the experiments. All experiments were done by. X.T., T.X. and J.L. X.T., T.X., and M.L.K. wrote the paper. M.L.K. and J.Z. edited the manuscript. All authors were given the opportunity to review the results and comment the manuscript.

References

Abdel-Banat, B.M., Hoshida, H., Ano, A., Nonklang, S., Akada, R., 2010. High-temperature fermentation: how can processes for ethanol production at high temperatures become superior to the traditional process using mesophilic yeast? Appl. Microbiol. Biotechnol. 85, 861–867.
Arsène, F., Tomoyasu, T., Bukau, B., 2000. The heat shock response of Escherichia coli. Int. J. Food Microbiol. 55, 3–9.
Asztalos, A., Daniels, M., Sethi, A., Shen, T., Langan, P., Redondo, A., Gnanakaran, S., 2012. A coarse-grained model for synergistic action of multiple enzymes on cellulose. Biotechnol. Biofuels 5, 55.
Bayer, E.A., Lamed, R., 1986. Ultrastructure of the cell surface cellulosome of Clostridium thermocellum and its interaction with cellulose. J. Bacteriol. 167, 828–836.
Bindea, G., Galon, J., Mlecnik, B., 2013. CluePedia Cytoscape plugin: pathway insights using integrated experimental and in silico data. Bioinformatics 29, 661–663.
Bindea, G., Mlecnik, B., Hackl, H., Charoentong, P., Tosolini, M., Kirilovsky, A., Fridman, W.-H., Pagès, F., Trajanoski, Z., Galon, J., 2009. ClueGO: a Cytoscape plug-in to decipher functionally grouped gene ontology and pathway annotation networks. Bioinformatics 25, 1091–1093.
Blouzard, J.C., Coutinho, P.M., Fierobe, H.P., Henrissat, B., Lignon, S., Tardif, C., Pagès, S., de Philip, P., 2010. Modulation of cellulosome composition in Clostridium cellulolyticum: adaptation to the polysaccharide environment revealed by proteomic and carbohydrate-active enzyme analyses. Proteomics 10, 541–554.
Charoensuk, K., Sakurada, T., Tokiyama, A., Murata, M., Kosaka, T., Thanonkeo, P., Yamada, M., 2017. Thermotolerant genes essential for survival at a critical high temperature in thermotolerant ethanologenic Zymomonas mobilis TISTR 548. Biotechnol. Biofuels 10, 204.
Chhabra, S., He, Q., Huang, K., Gaucher, S., Alm, E., He, Z., Hadi, M., Hazen, T., Wall, J., Zhou, J., 2006. Global analysis of heat shock response in Desulfovibrio vulgaris Hildenborough. J. Bacteriol. 188, 1817–1828.
Chu, E.K., Kilic, O., Cho, H., Groisman, A., Levchenko, A., 2018. Self-induced mechanical stress can trigger biofilm formation in uropathogenic Escherichia coli. Nat. Commun. 9, 4087.
Conesa, A., Gotz, S., Garcia-Gomez, J.M., Terol, J., Talon, M., Robles, M., 2005. Blast2GO: a universal tool for annotation, visualization and analysis in functional genomics research. Bioinformatics 21, 3674–3676.
Cui, G.-z., Hong, W., Zhang, J., Li, W.-l., Feng, Y., Liu, Y.-j., Cui, Q., 2012. Targeted gene engineering in Clostridium cellulolyticum H10 without methylation. J. Microbiol. Methods 89, 201–208.
Desvaux, M., 2005a. The cellulosome of Clostridium cellulolyticum. Enzym. Microb. Technol. 37, 373–385.
Desvaux, M., 2005b. Clostridium cellulolyticum: model organism of mesophilic cellulolytic clostridia. FEMS Microbiol. Rev. 29, 741–764.
Desvaux, M., Guedon, E., Petitdemange, H., 2000. Cellulose catabolism by Clostridium cellulolyticum growing in batch culture on defined medium. Appl. Environ. Microbiol. 66, 2461–2470.
Ferdinand, P.-H., Borne, R., Trotter, V., Pagès, S., Tardif, C., Fierobe, H.-P., Perret, S., 2013. Are cellulosome scaffolding protein CipC and CBM3-containing protein HycP, involved in adherence of Clostridium cellulolyticum to cellulose? PloS One 8.
Gal, L., Pages, S., Gaudin, C., Belaich, A., Reverbel-Leroy, C., Tardif, C., Belaich, J.-P., 1997. Characterization of the cellulolytic complex (cellulosome) produced by Clostridium cellulolyticum. Appl. Environ. Microbiol. 63, 903–909.
Giallo, J., Gaudin, C., Belaich, J., Petitdemange, E., Caillet-Mangin, F., 1983. Metabolism of glucose and cellobiose by cellulolytic mesophilic Clostridium sp. strain H10. Appl. Environ. Microbiol. 45, 843–849.
Guedon, E., Desvaux, M., Petitdemange, H., 2002. Improvement of cellulolytic properties of Clostridium cellulolyticum by metabolic engineering. Appl. Environ. Microbiol. 68, 53–58.
Guedon, E., Payot, S., Desvaux, M., Petitdemange, H., 1999. Carbon and electron flow in Clostridium cellulolyticum grown in chemostat culture on synthetic medium. J.

Bacteriol. 181, 3262–3269.
He, Z.L., Zhou, J.Z., 2008. Empirical evaluation of a new method for calculating signal-to-noise ratio for microarray data analysis. Appl. Environ. Microbiol. 74, 2957–2966.
Hemme, C.L., Fields, M.W., He, Q., Deng, Y., Lin, L., Tu, Q., Mouttaki, H., Zhou, A., Feng, X., Zuo, Z., 2011. Correlation of genomic and physiological traits of Thermoanaerobacter species with biofuel yields. Appl. Environ. Microbiol. 77, 7998–8008.
Hendriks, A., Zeeman, G., 2009. Pretreatments to enhance the digestibility of lignocellulosic biomass. Bioresour. Technol. 100, 10–18.
Higashide, W., Li, Y., Yang, Y., Liao, J.C., 2011. Metabolic engineering of Clostridium cellulolyticum for production of isobutanol from cellulose. Appl. Environ. Microbiol. 77, 2727–2733.
Jarvis, M., 2003. Cellulose stacks up. Nature 426, 611–612.
Jennert, K.C., Tardif, C., Young, D.I., Young, M., 2000. Gene transfer to Clostridium cellulolyticum ATCC 35319. Microbiology 146, 3071–3080.
Li, D.-C., Yang, F., Lu, B., Chen, D.-F., Yang, W.-J., 2012a. Thermotolerance and molecular chaperone function of the small heat shock protein HSP20 from hyperthermophilic archaeon, Sulfolobus solfataricus P2. Cell Stress Chaperones 17, 103–108.
Li, Y., Tschaplinski, T.J., Engle, N.L., Hamilton, C.Y., Rodriguez, M., Liao, J.C., Schadt, C.W., Guss, A.M., Yang, Y., Graham, D.E., 2012b. Combined inactivation of the Clostridium cellulolyticum lactate and malate dehydrogenase genes substantially increases ethanol yield from cellulose and switchgrass fermentations. Biotechnol. Biofuels 5, 2.
Li, Y., Xu, T., Tschaplinski, T.J., Engle, N.L., Yang, Y., Graham, D.E., He, Z., Zhou, J., 2014. Improvement of cellulose catabolism in Clostridium cellulolyticum by sporulation abolishment and carbon alleviation. Biotechnol. Biofuels 7, 25.
Liao, J.C., Mi, L., Pontrelli, S., Luo, S., 2016. Fuelling the future: microbial engineering for the production of sustainable biofuels. Nat. Rev. Microbiol. 14, 288.
Lynd, L.R., Cushman, J.H., Nichols, R.J., Wyman, C.E., 1991. Fuel ethanol from cellulosic biomass. Science 251, 1318–1323.
Lynd, L.R., Van Zyl, W.H., McBride, J.E., Laser, M., 2005. Consolidated bioprocessing of cellulosic biomass: an update. Curr. Opin. Biotechnol. 16, 577–583.
Maamar, H., Abdou, L., Boileau, C., Valette, O., Tardif, C., 2006. Transcriptional analysis of the cip-cel gene cluster from Clostridium cellulolyticum. J. Bacteriol. 188, 2614–2624.
Miller, G.L., 1959. Use of dinitrosalicylic acid reagent for determination of reducing sugar. Anal. Chem. 31, 426–428.
Mingardon, F., Bagert, J.D., Maisonnier, C., Trudeau, D.L., Arnold, F.H., 2011. Comparison of family 9 cellulases from mesophilic and thermophilic bacteria. Appl. Environ. Microbiol. 77, 1436–1442.
Murata, M., Fujimoto, H., Nishimura, K., Charoensuk, K., Nagamitsu, H., Raina, S., Kosaka, T., Oshima, T., Ogasawara, N., Yamada, M., 2011. Molecular strategy for survival at a critical high temperature in Escherichia coli. PloS One 6, e20063.
Payot, S., Guedon, E., Cailliez, C., Gelhaye, E., Petitdemange, H., 1998. Metabolism of cellobiose by Clostridium cellulolyticum growing in continuous culture: evidence for decreased NADH reoxidation as a factor limiting growth. Microbiology 144, 375–384.
Ritchie, M.E., Phipson, B., Wu, D., Hu, Y.F., Law, C.W., Shi, W., Smyth, G.K., 2015. Limma powers differential expression analyses for RNA-sequencing and microarray studies. Nucleic Acids Res. 43.
Soemphol, W., Deeraksa, A., Matsutani, M., Yakushi, T., Toyama, H., Adachi, O., Yamada, M., Matsushita, K., 2011. Global analysis of the genes involved in the thermotolerance mechanism of thermotolerant Acetobacter tropicalis SKU1100. Biosc. Biotech. Biochem. 1108312638 1108312638.
Tachaapaikoon, C., Kosugi, A., Pason, P., Waeonukul, R., Ratanakhanokchai, K., Kyu, K.L., Arai, T., Murata, Y., Mori, Y., 2012. Isolation and characterization of a new cellulosome-producing Clostridium thermocellum strain. Biodegradation 23, 57–68.
Tamaru, Y., Miyake, H., Kuroda, K., Ueda, M., Doi, R.H., 2010. Comparative genomics of the mesophilic cellulosome-producing Clostridium cellulovorans and its application to biofuel production via consolidated bioprocessing. Environ. Technol. 31, 889–903.
Vasu, K., Nagaraja, V., 2013. Diverse functions of restriction-modification systems in addition to cellular defense. Microbiol. Mol. Biol. Rev. 77, 53–72.
Venables, W.N., Ripley, B.D., 2013. Modern Applied Statistics with S-PLUS. Springer Science & Business Media.
Xu, C., Huang, R., Teng, L., Jing, X., Hu, J., Cui, G., Wang, Y., Cui, Q., Xu, J., 2015a. Cellulosome stoichiometry in Clostridium cellulolyticum is regulated by selective RNA processing and stabilization. Nat. Commun. 6, 6900.
Xu, T., Li, Y., Shi, Z., Hemme, C.L., Li, Y., Zhu, Y., Van Nostrand, J.D., He, Z., Zhou, J., 2015b. Efficient genome editing in Clostridium cellulolyticum via CRISPR-Cas9 nickase. Appl. Environ. Microbiol. 81, 4423–4431.
Zhang, Y.-H.P., Himmel, M.E., Mielenz, J.R., 2006. Outlook for cellulase improvement: screening and selection strategies. Biotechnol. Adv. 24, 452–481.
Zhang, Y.P., Hong, J., Ye, X., 2009. Cellulase Assays. Biofuels. Springer, pp. 213–231.